CO_2 Laser irradiation of GeO_2 planar waveguide fabricated by rf-sputtering

A. Chiasera,[1,*] C. Macchi,[2] S. Mariazzi,[3] S. Valligatla,[1,4,5] L. Lunelli,[6] C. Pederzolli,[7] D.N. Rao,[4] A. Somoza,[8] R.S. Brusa,[9] and M. Ferrari[1]

[1]*CNR-IFN CSMFO Lab, Via alla Cascata 56/C, Povo, 38123 Trento, Italy*
[2]*IFIMAT, UNCentro and CONICET, Pinto 399, B7000GHG Tandil, Argentina*
[3]*Dipartimento di Fisica, Università di Trento and INFN, Gruppo collegato di Trento, Via Sommarive 14, I-38123 Povo, Trento, Italy*
[4]*School of Physics, University of Hyderabad, Hyderabad 500046, India.*
[5]*Università di Trento, Dipartimento di Fisica, via Sommarive 14, Povo, 38123 Trento, Italy*
[6]*Bruno Kessler Foundation and National Research Council Institute of Biophysics, via Sommarive 18, Trento Italy*
[7]*Bruno Kessler Foundation, via Sommarive 18, Trento Italy*
[8]*IFIMAT, UNCentro and CICPBA, Pinto 399, B7000GHG Tandil, Argentina*
[9]*Dipartimento di Fisica and CNISM, Università di Trento, Via Sommarive 14, I-38123 Trento, Italy*
**achiaser@science.unitn.it*

Abstract: GeO_2 transparent glass ceramic planar waveguides were fabricated by a RF-sputtering technique and then irradiated by a pulsed CO_2 laser. The effects of CO_2 laser processing on the optical and structural properties of the waveguides were evaluated by different techniques including m-line, micro-Raman spectroscopy, atomic force microscopy, and positron annihilation spectroscopy. After laser annealing, an increase of the refractive index of approximately 0.04 at 1.5 μm and a decrease of the attenuation coefficient from 0.9 to 0.5 db/cm at 1.5 μm was observed. Raman spectroscopy and microscopy results put in evidence that the system embeds GeO_2 nanocrystals and their phase varies with the irradiation time. Moreover, positron annihilation spectroscopy was used to study the depth profiling of the as prepared and laser annealed samples. The obtained results yielded information on the structural changes produced after the irradiation process inside the waveguiding films of approximately 1 μm thickness. In addition, a density value of the amorphous GeO_2 samples was evaluated.

OCIS codes: (140.3390) Laser materials processing; (310.1860) Deposition and fabrication; (160.4760) Optical properties; (300.6450) Spectroscopy, Raman; (300.6250) Spectroscopy, condensed matter; (310.2790) Guided waves.

References and links

1. C. V. Ramana, G. Carbajal-Franco, R. S. Vemuri, I. B. Troitskaia, S. A. Gromilov, and V. V. Atuchin, "Optical properties and thermal stability of germanium oxide (GeO_2) nanocrystals with α-quartz structure," Mater. Sci. Eng. B-Adv. Funct. Solid-State Mater. **174**(1-3), 279–284 (2010).
2. N. Terakado and K. Tanaka, "Photo-induced phenomena in sputtered GeO_2 films," J. Non-Cryst. Solids **351**(1), 54–60 (2005).
3. Y. Su, X. Liang, S. Li, Y. Chen, Q. Zhou, S. Yin, X. Meng, and M. Kong, "Self-catalytic VLS growth and optical properties of single-crystalline GeO_2 nanowire arrays," Mater. Lett. **62**(6-7), 1010–1013 (2008).
4. C. Ferrante, E. Pontecorvo, G. Cerullo, A. Chiasera, G. Ruocco, W. Schirmacher, and T. Scopigno, "Acoustic dynamics of network-forming glasses at mesoscopic wavelengths," Nat Commun **4**, 1793-1–1793- 6 (2013).
5. A. Chiasera, G. Alombert-Goget, M. Ferrari, S. Berneschi, S. Pelli, B. Boulard, and C. D. Arfuso, "Rare earth–activated glass-ceramic in planar format," Opt. Eng. **50**, 071105–1–071105–10 (2011).
6. V. P. Prakapenk, G. Shen, L. S. Dubrovinsky, M. L. Rivers, and S. R. Sutton, "High pressure induced phase transformation of SiO_2 and GeO_2: difference and similarity," J. Phys. Chem. Solids **65**, 1537–1545 (2004).
7. S. Berneschi, S. Soria, G. C. Righini, G. Alombert-Goget, A. Chiappini, A. Chiasera, Y. Jestin, M. Ferrari, S. Guddala, E. Moser, S. N. B. Bhaktha, B. Boulard, C. D. Arfuso, and S. Turrell, "Rare-earth-activated glass–ceramic waveguides," Opt. Mater. **32**(12), 1644–1647 (2010).

#190596 - $15.00 USD Received 16 May 2013; revised 8 Jul 2013; published 30 Aug 2013

8. B. Boulard, G. Alombert, I. Savelii, C. D. Arfuso, Y. Gao, M. Ferrari, and F. Prudenzano, "Er/Yb^{3+}/Ce^{3+} co-doped fluoride glass ceramics waveguides for application in the 1.5 μm telecommunication window," Advances in Science and Technology **71**, 16–21 (2010).
9. A. Chiasera, C. Armellini, S. N. B. Bhaktha, A. Chiappini, Y. Jestin, M. Ferrari, E. Moser, A. Coppa, V. Foglietti, P. T. Huy, K. Tran Ngoc, G. Nunzi Conti, S. Pelli, G. C. Righini, and G. Speranza, "Er^{3+}/Yb^{3+}-activated silica-hafnia planar waveguides for photonics fabricated by rf-sputtering," J. Non-Cryst. Solids **355**(18-21), 1176–1179 (2009).
10. G. Nunzi Conti, S. Berneschi, M. Brenci, S. Pelli, S. Sebastiani, G. C. Righini, C. Tosello, A. Chiasera, and M. Ferrari, "UV photoimprinting of channel waveguides on active SiO2–GeO2 sputtered thin films," Appl. Phys. Lett. **89**, 121102–1–121102–3 (2006).
11. S. Valligatla, A. Chiasera, S. Varas, N. Bazzanella, D. N. Rao, G. C. Righini, and M. Ferrari, "High quality factor 1-D Er^{3+}-activated dielectric microcavity fabricated by rf-sputtering," Opt. Express **20**(19), 21214–21222 (2012).
12. M. Zevin and R. Reisfeld, "Preparation and properties of active waveguides based on zirconia glasses," Opt. Mater. **8**(1-2), 37–41 (1997).
13. S. Dutta, H. E. Jackson, J. T. Boyd, R. L. Davis, and F. S. Hickernell, "CO_2 laser annealing of Si_3N_4, Nb_2O_5 and Ta_2O_5 thin-film optical waveguides to achieve scattering loss reduction," IEEE J. Quantum Electron. **18**, 800–806 (1982).
14. C. Goyes, M. Ferrari, C. Armellini, A. Chiasera, Y. Jestin, G. C. Righini, F. Fonthal, and E. Solarte, "CO_2 laser annealing on erbium-activated glass–ceramic waveguides for photonics," Opt. Mater. **31**(9), 1310–1314 (2009).
15. S. Dutta, H. E. Jackson, and J. T. Boyd, "Reduction of scattering from a glass thin-film optical waveguide by CO_2 laser annealing," Appl. Phys. Lett. **37**(6), 512–514 (1980).
16. S. Dutta, H. E. Jackson, and J. T. Boyd, "Extremely low-loss glass thin-film optical waveguides utilizing surface coating and laser annealing," J. Appl. Phys. **52**(6), 3873–3875 (1981).
17. S. Dutta, H. E. Jackson, J. T. Boyd, F. S. Hickernell, and R. L. Davis, "Scattering loss reduction in ZnO optical waveguides by laser annealing," Appl. Phys. Lett. **39**(3), 206–208 (1981).
18. Q. Liu, K. S. Chiang, L. Reekie, and Y. T. Chow, "CO_2 laser induced refractive index changes in optical polymers," Opt. Express **20**(1), 576–582 (2012).
19. A. Obata, J. R. Jones, A. Shinya, and T. Kasuga, "Sintering and crystallization of phosphate glasses by CO_2-laser irradiation on hydroxyapatite ceramics," Int. J. Appl. Ceram. Technol. **9**(3), 541–549 (2012).
20. N. Jiang, J. Qiu, and J. C. H. Spence, "Precipitation of Ge nanoparticles from GeO2 glasses in transmission electron microscope," Appl. Phys. Lett. **86**, 143112–1–143112–3 (2005).
21. P. Muller-Buschbaum, "A basic introduction to grazing incidence small-angle X-ray scattering," Lect. Notes Phys. **776**, 61–89 (2009).
22. P. Coleman, *Positron Beams and Their Applications* (World Scientific, Singapore, 2000).
23. S. J. L. Ribeiro, Y. Messaddeq, R. R. Gonçalves, M. Ferrari, M. Montagna, and M. A. Aegerter, "Low optical loss planar waveguides prepared by an organic-inorganic hybrid system," Appl. Phys. Lett. **77**(22), 3502–3504 (2000).
24. C. A. Schneider, W. S. Rasband, and K. W. Eliceiri, "NIH Image to ImageJ: 25 years of image analysis," Nat. Methods **9**(7), 671–675 (2012).
25. A. Zecca, M. Bettonte, J. Paridaens, G. P. Karwasz, and R. S. Brusa, "A new electrostatic positron beam for surface studies," Meas. Sci. Technol. **9**(3), 409–416 (1998).
26. C. Macchi, S. Mariazzi, G. P. Karwasz, R. S. Brusa, P. Folegati, S. Frabboni, and G. Ottaviani, "Single-crystal silicon coimplanted by helium and hydrogen: evolution of decorated vacancylike defects with thermal treatments," Phys. Rev. B **74**(17), 174120 (2006).
27. R. S. Brusa, G. P. Karwasz, N. Tiengo, A. Zecca, F. Corni, R. Tonini, and G. Ottaviani, "Formation of vacancy clusters and cavities in He-implanted silicon studied by slow-positron annihilation spectroscopy," Phys. Rev. B **61**(15), 10154–10166 (2000).
28. P. Schultz and K. G. Lynn, "Interaction of positron beams with surfaces, thin films, and interfaces," Rev. Mod. Phys. **60**(3), 701–779 (1988).
29. S. Valkealahti and R. M. Nieminen, "Monte Carlo calculations of keV electron and positron slowing down in solids. II," Appl. Phys., A Mater. Sci. Process. **35**(1), 51–59 (1984).
30. P. Asoka-Kumar, K. G. Lynn, and D. O. Welch, "Characterization of defects in Si and SiO_2–Si using positrons," J. Appl. Phys. **76**(9), 4935–4982 (1994).
31. A. Trukhin and B. Capoen, "Raman and optical reflection spectra of germanate and silicate glasses," J. Non-Cryst. Solids **351**(46-48), 3640–3643 (2005).
32. C. Duverger, S. Turrell, M. Bouazaoui, F. Tonelli, M. Montagna, and M. Ferrari, "Preparation of SiO_2-GeO_2:Eu^{3+} planar waveguides and characterisation by waveguide Raman and luminescence spectroscopies," Philos. Mag. B **77**(2), 363–372 (1998).
33. Y. M. Yang, L. W. Yang, and P. K. Chu, "Polarized Raman scattering of Ge nanocrystals embedded in a-SiO2," Appl. Phys. Lett. **90**, 081909-1–081909-3 (2007).
34. T. P. Mernagh and L. G. Liu, "Temperature dependence of Raman spectra of the quartz- and rutile-types of GeO_2," Phys. Chem. Miner. **24**(1), 7–16 (1997).

#190596 - $15.00 USD Received 16 May 2013; revised 8 Jul 2013; published 30 Aug 2013

35. V. V. Atuchin, T. A. Gavrilova, S. A. Gromilov, V. G. Kostrovsky, L. D. Pokrovsky, I. B. Troitskaia, R. S. Vemuri, G. Carbajal-Franco, and C. V. Ramana, "Low-temperature chemical synthesis and microstructure analysis of GeO_2 crystals with α-quartz structure," Cryst. Growth Des. **9**(4), 1829–1832 (2009).
36. M. Madon, P. Gillet, C. Julien, and G. D. Price, "A vibrational study of phase transitions among the GeO_2 polymorphs," Phys. Chem. Miner. **18**(1), 7–18 (1991).
37. R. G. Hunsperger, *Integrated Optics – Theory and Technology* (Springer-Verlag 2009), Chap. 6.
38. S. Berneschi, S. Soria, G. C. Righini, G. Alombert-Goget, A. Chiappini, A. Chiasera, Y. Jestin, M. Ferrari, S. Guddala, E. Moser, S. N. B. Bhaktha, B. Boulard, C. D. Arfuso, and S. Turrell, "Rare-earth-activated glass–ceramic waveguides," Opt. Mater. **32**(12), 1644–1647 (2010).
39. A. Van Veen, H. Schut, J. de Vries, R. A. Hakvoort, and M. R. Ijpma, "Analysis of positron profiling data by means of VEPFIT," AIP Conf. Proc. **218**, 171–198 (1991).
40. P. Hermet, G. Fraysse, A. Lignie, P. Armand, and P. Papet, "Density functional theory predictions of the nonlinear optical properties in α-Quartz-type germanium dioxide," J. Phys. Chem. C **116**(15), 8692–8698 (2012).
41. Q. Liu, Z. Liu, L. Feng, and H. Tian, "First-principles study of structural, elastic, electronic and optical properties of rutile GeO_2 and a-quartz GeO_2," Solid State Sci. **12**(10), 1748–1755 (2010).
42. J. Lucas, "Infrared glasses," Curr. Opin. Solid State Mater. Sci. **4**(2), 181–187 (1999).
43. D. W. Sheibley and M. H. Fowler, "Infrared spectra of Various metal oxides in the region of 2 to 26 microns. NASA TN D-3750," Tech. Note U. S. Natl. Aeronaut. Space Adm. **D-3750**, 1–62 (1967).
44. T. Hidaka, K. Kumada, J. Shimada, and T. Morikawa, "GeO_2-ZnO-K_2O glass as the cladding material of 940 cm^{-1} CO_2 laser-light transmitting hollow-core waveguide," J. Appl. Phys. **53**(8), 5484–5490 (1982).

1. Introduction

The growth, characterization, and employment of GeO_2 for application in modern electronic and optical devices continue to be an interesting topic for theoretical and experimental investigations [1]. GeO_2 exhibits many interesting physicochemical properties for applications in optical, electronic and optoelectronic devices [1–3], and very recently GeO_2 films have been employed as a prototypical case for the study for hypersonic attenuation in a strong glass [4]. In fact, GeO_2 can give photoluminescence, exhibits high values of dielectric constant and refractive index, and good thermal stability and mechanical strength. Photo-sensor capability of GeO_2 has been confirmed by optical spectroscopic methods such as Raman-spectroscopy and electron spin resonance spectroscopy coupled with structural measurements [2]. Moreover, nanocomposite materials such as transparent glass ceramics have been demonstrated to exhibit specific optical and structural properties making them valuable photonic systems [5]. For these reasons, it is of technological and scientific importance to develop fabrication protocols to obtain GeO_2 transparent glass ceramic planar waveguides exhibiting low attenuation coefficients and simultaneously embed GeO_2 nanocrystals with a specific phase [6].

Various techniques can be used to fabricate these particular kinds of nanostructured systems [5]. Among them, sol-gel techniques with top-down and bottom-up approaches [7], and physical vapor deposition [8]. In recent years, we have demonstrated that RF- sputtering (RFS) is a suitable technique to fabricate optical planar waveguides and photonic microcavities operating in the visible and NIR regions [9–11].

In order to produce transparent glass-ceramic, heat treatment employing a furnace is currently used, but recently efforts were performed for the development of alternative treatments like the laser annealing (LA) process especially for its advantages in terms of temporal and spatial annealing control [12–14]. The CO_2 laser annealing has been successfully used to reduce scattering losses in different kinds of amorphous optical planar waveguides [15–18], and for the fabrication of glass-ceramic coating [19] and glass-ceramic waveguides with low attenuation coefficient [14].

The characterization of the structure of the samples is crucial to assess the effect of the LA process and to determine the appropriate irradiation protocols. However, it is well known that important structural modification, leading to artificial results, can be induced in GeO_2 based materials by electron irradiation [20] and analysis techniques such as Grazing Incidence Small-Angle X-Ray Scattering [21] need to be complemented with other investigations to be exhaustive for low volume scattering systems. For these reasons, in the present work information on the structural properties of the waveguides before and after the laser annealing

#190596 - $15.00 USD Received 16 May 2013; revised 8 Jul 2013; published 30 Aug 2013

process were obtained from positron annihilation spectroscopy (PAS), specifically by Doppler broadening spectroscopy (DBS). PAS is a well-recognized non-destructive spectroscopy technique employed to investigate materials structure [22].

In this work we present the fabrication by RF-sputtering of amorphous GeO_2 planar waveguides, their modification in glass-ceramic by CO_2 laser annealing, and the optical and structural characterization of the samples before and after irradiation.

2. Experimental

GeO_2 planar waveguides were prepared by a Radio Frequency Sputtering (RFS) technique. The film was deposited on a silica substrate of dimensions 7.5 x 2.5 cm. In order to improve the adhesion of the films, just before the deposition procedure the substrate was cleaned inside the deposition chamber by heating at 120 °C for 30 min. Sputtering deposition of the film was performed by using a 15x3 cm^2 germania target. The residual pressure, before deposition, was about $1.6x10^{-6}$ mbar. The substrates were not heated during the deposition process. The sputtering was carried out under an Ar atmosphere at a pressure of $5.4x10^{-3}$ mbar without addition of oxygen, an applied rf power of 80 W, and 0 W reflected power. The deposition time, necessary to reach the appropriate thickness for one propagating mode at 1.5 μm, was 1 h 58 min.

The GeO_2 planar waveguides were irradiated with a pulsed S50 TEA CO_2 laser with a mixture of CO_2:N_2:He fixed at 33%:33%:33%, respectively. The pulsed laser was used with 0.6 J per pulse at 5 Hz repetition rate and 380 ns pulse width, 10.6 μm wavelength and a beam diameter of 1.5 cm. The samples were irradiated in air with 1.3 W medium power and the irradiation times varied from 1 h to 2 h.

The thickness of the waveguide and the refractive index at 543.5, 632.8, 1319 and 1542 nm were measured in TE and TM polarizations, by an m-line apparatus based on the prism coupling technique. Using the same apparatus, attenuation coefficients at 632.8, 1319 and 1542 nm were evaluated by collecting with a fiber scanner the light scattered out of the waveguide plane for the TE_0 mode. More details about the experimental setup can be found in Ref [23].

Raman scattering measurements were performed at room temperature in the range between 100 and 1000 cm^{-1} by means of a microprobe setup (Horiba-Jobin-Yvon, LabRam Aramis) consisting of a He-Ne laser operating at 632.8 nm with 20 mW power, a narrow band notch filter, a 46 cm focal length spectrograph using a 1800 grooves/mm grating and a charge-coupled device (CCD) detector. Exciting radiation at 632.8 nm was focused onto the sample surface with a spot size of about 1 μm^2 through a 100X objective with NA = 0.9. To avoid unwanted laser-induced transformations, neutral filters of different optical densities were used, whenever necessary. The resolution was about 0.35 cm^{-1}/pixel.

AFM measurements were performed using a Solver AFM (NT-MDT, Russia) in contact mode in air using a 50 μm scanner. CSG11 silicon cantilevers from NT-MDT with nominal force constant of 0.1 N/m were used. Images of different sample areas were acquired, ranging from 1x1 to 7.5x7.5 μm^2. The data were processed with Gwyddion v. 2.30 (www.gwyddion.net), applying plane correction and line-by-line leveling. The same software was used to apply correction factors obtained using a calibration grid (TGQ1, NT-MDT) and to compute data roughness average (R_a). Data were imaged using ImageJ [24].

Compositional analyses were performed using Energy Dispersive X-ray Spectroscopy (EDXS) technique, employing an Oxford INCA PentaFETx3 apparatus. The EDXS instrument is mounted on a JEOL Scanning Electron Microscope (SEM) JSM-7001F equipped with a Field Effect Gun (FEG) source.

DBS measurements were carried out with an electrostatic slow positron beam at Trento University [25, 26]. The beam was tunable in the 0.05–25 keV energy range. In GeO_2, these positron implantation energies correspond to a probed film thickness ranging from about 0.1 nm to approximately 2 μm. The positron beam was coupled to two high purity germanium

#190596 - $15.00 USD Received 16 May 2013; revised 8 Jul 2013; published 30 Aug 2013

detectors (HPGe), 45% efficiency, 1.4 keV resolution at 511 keV, in a 180° configuration. At each positron implantation energy, the 511 keV gamma line was acquired with a microspectrum method and stabilized by a software procedure [27].

Positrons injected in a solid with energy ranging from a few eV to some keV slow down in few picoseconds (1-3 ps at 300 K) reaching thermal energy with the material. Then, after a diffusion path, positrons become efficiently trapped in open volumes and there they annihilate with electrons. The high specific trapping rate of positrons for open volumes present in a solid makes this particle a very efficient non-destructive probe for characterizing variations in structural open volumes or defects from monovacancies up to voids. The annihilation characteristics are determined by the local electron environment of the annihilation site (i.e., positron trap) [28].

For monoenergetic positrons, the stopping profile can be well-described by a derivative of a Gaussian function [29, 30]. The mean positron implantation depth $< z >$ is related to the positron implantation energy E by the equation:

$$< z >= \frac{40}{\rho} E^{1.6}\ nm \qquad (1)$$

where E is expressed in keV and the material density ρ in g/cm^3.

When using DBS, the 511 keV annihilation peak is usually characterized by the line shape parameter S. This parameter represents the fraction of positrons annihilating with low-momentum electrons and is defined as the ratio between the counts in a central area of the annihilation peak ($\left|511 - E_\gamma\right| \le 0.85 keV$) and the counts in the total area of the photopeak ($\left|511 - E_\gamma\right| \le 4.25 keV$). In the parentheses the energy regions of the annihilation peak used in the present experiment are reported. E_γ is the energy of the annihilation photon.

The narrowing of the 511 keV annihilation line indicates that more positrons are annihilating with electrons of low momentum; this behavior is reflected in an increase of the S values.

From the DBS spectra the S parameter was estimated with a statistical error of about 0.1% (more than 2.5×10^5 counts under each annihilation spectrum).

Usually, to analyze DBS data, the shape line parameter is normalized to that of a reference bulk (S_b) material; that is $S_n = S/S_b$. In this work, as reference was used the S_b of the silica substrate.

3. Results and discussions

The samples are planar waveguides with dimension 7.5 x 2.5 cm. The light propagates in a GeO_2 film with thickness of 1.0 ± 0.1 μm.

In Table 1 are reported the optical parameters for the samples as prepared and after CO_2 laser irradiation for 2h.

Table 1. Optical parameters for the samples as prepared and after CO_2 laser irradiation for 2h.

Laser wavelength (nm)		Refractive Index		thickness (μm)	Attenuation coefficient (dB/cm)
		TE	TM		
632	before irradiation	1.614 ± 0.001	1.616 ± 0.001	1.1 ± 0.1	1.9 ± 0.2
	after irradiation	1.652 ± 0.001	1.653 ± 0.001	1.1 ± 0.1	1.1 ± 0.2
1319	before irradiation	1.590 ± 0.01	1.590 ± 0.01	1.0 ± 0.1	1.4 ± 0.2
	after irradiation	1.631 ± 0.01	1.634 ± 0.01	1.0 ± 0.1	0.7 ± 0.2
1542	before irradiation	1.585 ± 0.01	1.585 ± 0.01	1.0 ± 0.1	0.9 ± 0.2
	after irradiation	1.623 ± 0.01	1.624 ± 0.01	1.0 ± 0.1	0.5 ± 0.2

#190596 - $15.00 USD Received 16 May 2013; revised 8 Jul 2013; published 30 Aug 2013

The waveguides have a thickness of about 1μm and support one mode at 1319 nm and 1542 nm. No change in the overall thickness was evidenced after the laser irradiation by the m-line measurements. Before and after LA the refractive indices measured in TE and TM polarization modes are equal within the experimental uncertainty, so the birefringence can be considered negligible. Comparing the refractive indices in the GeO_2 waveguides before and after LA we observe an increase of about 0.04 with the irradiation at all the wavelengths. Similar variations were obtained in other systems treated by CO_2 LA [14]. The laser annealing allowed significant reduction of the attenuation coefficients. In fact, we observe an attenuation coefficient at 1542 nm of 0.5 dB/cm for the irradiated system while for the system before LA is 0.9 dB/cm. As shown in Table 1, the reduction of the attenuation coefficient with the CO_2 laser irradiation is present at all the considered wavelengths. The decrease in the total attenuation coefficient for the CO_2 laser irradiated systems, that take into account all the contribution to the losses such as volume and surface scattering and absorption, has been attributed by Dutta et al. [16] to the reduction of the surface roughness. The optical parameters measured after 1h of LA are equivalent to those reported for 2h. EDXS analysis was used to monitor the chemical composition of the sample, as deposited and after LA. EDXS confirms that the composition of the sample is not affected by the laser irradiation and the correct stoichiometry between germanium and oxygen is always present.

In Fig. 1, the Micro Raman spectra measured at room temperature for GeO_2 planar waveguides before and after LA at different times are reported.

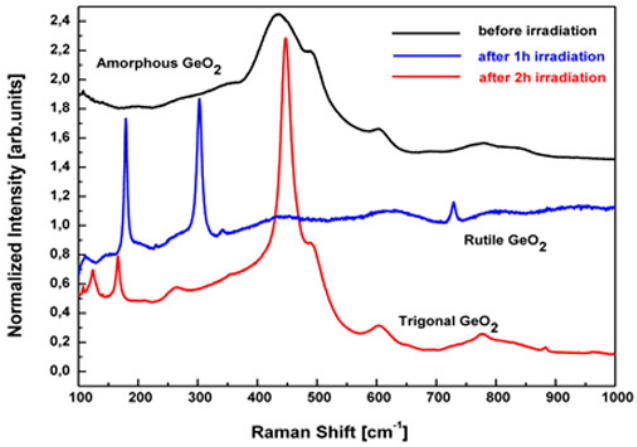

Fig. 1. Micro Raman measurements carried out at room temperature for GeO_2 planar waveguide.

The Raman spectrum of the as prepared GeO_2 waveguide before irradiation is typical of a GeO_2 amorphous system. The amorphous nature of the GeO_2 film is clearly pointed out by the broad peak at 440 cm^{-1} [31, 32]. After 1 h of CO_2 laser irradiation, the Raman spectra indicate that in the amorphous GeO_2 matrix there is the presence of a rutile-like GeO_2 crystalline phase. The observed peaks are, in fact, in good agreement with those reported in the literature [31]. The peak at 302 cm^{-1} corresponds to Ge optical phonons, being related to Ge–Ge bonds [33]. After 2 h of CO_2 laser irradiation, the Raman spectrum shows that in the amorphous system there is also the presence of a trigonal GeO_2 crystal phase. The peaks at 124, 168 and 263 cm^{-1} correspond, in fact to the complex translation and rotation of GeO_4 tetrahedra [34]. The peak at 882 cm^{-1} is assigned to Ge-O stretching motion with tetrahedral GeO_4 units [35]. A shift in the band at 444 cm^{-1} is due to symmetric Ge-O-Ge stretching [35]. The peaks

#190596 - $15.00 USD Received 16 May 2013; revised 8 Jul 2013; published 30 Aug 2013

observed at 490 and 603 cm^{-1} are D_1 and D_2 defect bands from the silica substrate. All the bands in the spectrum obtained for the GeO_2 waveguide after 2 h of CO_2 laser irradiation are in good agreement with those of GeO_2 calcinated under a temperature T = 1050 °C [36].

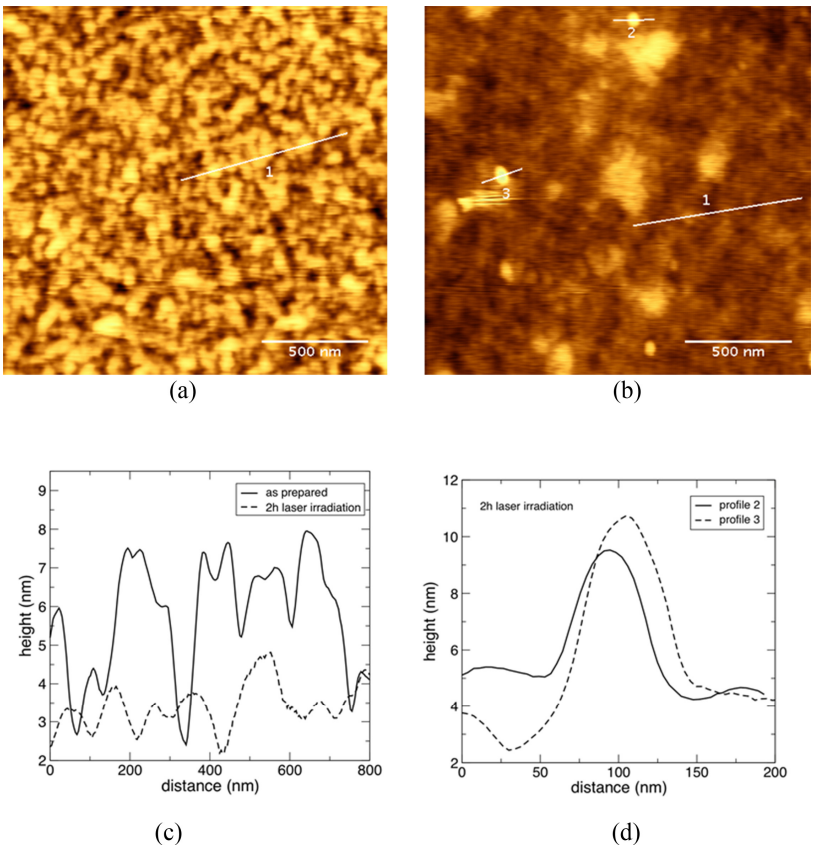

Fig. 2. AFM images of representative 1.8 x 1.8 μm^2 areas of the samples in the conditions: (a) as prepared and (b) after 2h of CO_2 laser irradiation. Z scale 10 nm. In (c) a comparison of typical height profiles in these two conditions, corresponding to sections 1 in panels (a) and (b), showing a decrease in roughness after irradiation is presented. (d) profiles of the nanometric structures found after irradiation - sections 2 and 3 in panel (b).

AFM images of representative 1.8 x 1.8 μm^2 areas for the as prepared sample and for that CO_2 laser irradiated for 2h are reported in Figs. 2(a) and 2(b) respectively. AFM analysis put in evidence a roughness of 1.05 ± 0.05 nm in the as prepared sample and a roughness of 0.80 ± 0.02 nm for the waveguide after 2h of CO_2 laser irradiation. This result correlates with the reduction of the attenuation coefficient with the laser annealing and confirms surface morphology as an important source of losses [37]. Moreover, on the surface of the sample, the AFM image of Fig. 2(b) shows the presence of nanometric structures with sizes ranging from 10 to 50 nm (see also Fig. 2 (c)).These structures are assigned to GeO_2 nanocrystals. It is worth noting that, although the presence of these scattering points are expected to increase the attenuation coefficient by increasing the scattering losses of the waveguide [38], the protocol here developed for the CO_2 irradiation allows reducing the attenuation coefficient by decreasing the surface scattering losses [17, 37].

In Fig. 3, the positron depth profiling obtained for the as prepared and for the 2h CO_2 laser irradiated GeO_2 waveguides samples are shown. Specifically, the normalized shape parameter S_n as a function of the positron implantation energy and of the positron mean implantation

#190596 - $15.00 USD Received 16 May 2013; revised 8 Jul 2013; published 30 Aug 2013

depth is shown. For sake of clarity, in Fig. 3 only two S_n evolutions are shown; i.e., the S_n curve corresponding to the 1h CO_2 laser irradiated sample was omitted.

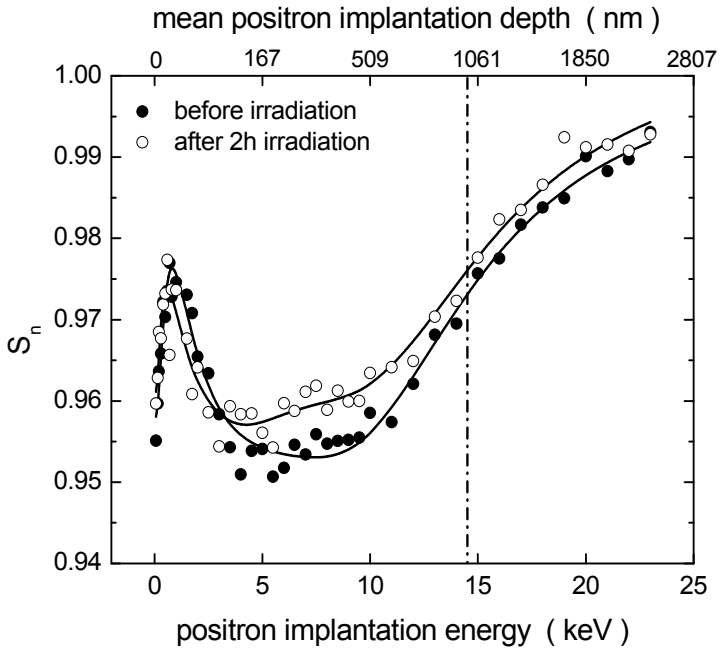

Fig. 3. Normalized shape parameter S_n as a function of the positron implantation energy for the as prepared and after 2h CO_2 laser irradiated GeO_2 samples. In the upper scale the mean positron implantation depth is reported. Solid lines represent the best fit obtained using the VEPFIT program (see text). The vertical dash-dotted line points out the interface limit between the film and the silica substrate.

To analyze the positron depth profiling of all the studied GeO_2 waveguides, the S_n(E) experimental data were fitted using a procedure based on the solution of the stationary positron diffusion equation (VEPFIT program [39]). The equation requires as an input the positron stopping profile. Experimental data obtained from the measurements of the as prepared film were well-fitted considering two layers plus the silica substrate. On the other hand, although no changes were observed by m-line measurements in the overall thickness of the waveguides, in the case of the irradiated samples it was found that the data of both waveguides could be satisfactorily fitted using three layers plus the silica substrate. To fit the positron depth profiles it is necessary to have the density of the different layers including that of the substrate (see relation between depth and density given in Eq. (1). For silica a density value of 2.1 g/cm^3 was assumed. However, taking advantage of having precise measurements of the layer thicknesses of each deposited Germania film as obtained using an m-line apparatus, the S_n versus E curves were analyzed considering the density values of the GeO_2 films of each sample as guess parameters. The GeO_2 density was found to be 3.15 ± 0.02 g/cm^3. A summary of the results is presented in Table 2. The fitted characteristic value of the silica substrate was S_b = 0.529 ± 0.001.

#190596 - $15.00 USD Received 16 May 2013; revised 8 Jul 2013; published 30 Aug 2013

Table 2. S_n values characterizing each layer in the as prepared and the two irradiated samples, as obtained by fitting the positron depth profiles. The density value of the GeO_2 film was used as a guess parameter into the frame of the fitting procedure. The boundary depths are measured from the surface of the sample.

Sample	layer I ρ = 3.15 g/cm^3		layer II ρ = 3.15 g/cm^3		layer III ρ = 3.15 g/cm^3		bulk ρ = 2.1 g/cm^3
	S_n	depth (nm)	S_n	depth (nm)	S_n	depth (nm)	S_n
before irradiation	1.006	11 ± 2	0.952	983 ± 20	–	–	1.000
after 1h irradiation	1.003	2 ± 0.2	0.946	320 ± 25	0.966	983	1.000
after 2h irradiation	0.980	5 ± 0.1	0.950	175 ± 32	0.960	983	1.000

In the as prepared film, positrons detect a first thin superficial layer of about 10 nm which is characterized by a very high S_n value of 1.006. This thin layer is followed by another GeO_2 layer (labelled layer II) uniform up to the silica substrate and characterized by a S_n = 0.952. With the laser irradiation, the superficial layer reduces to half of its initial thickness, and the uniform second layer observed in the as prepared film splits now into two regions, named layers II and III, respectively. The first region is structurally similar to the second layer of the non-irradiated sample having about the same S_n value (~0.950). In the sample irradiated during 1 h the thickness of the second layer is around 300 nm; and in the case of the sample irradiated 2 h, this thickness decreases up to approximately 170 nm. On the other hand, the second region (i.e., layer III) is characterized by a higher S_n value (~0.960) than the previous one and it extends up to the silica interface.

The structural changes in the GeO_2 films with the irradiation are illustrated in the scheme plotted in Fig. 4. For all the samples and the different layers we have obtained values of the positron diffusion length (L_+) ranging between 5 nm and 25 nm.

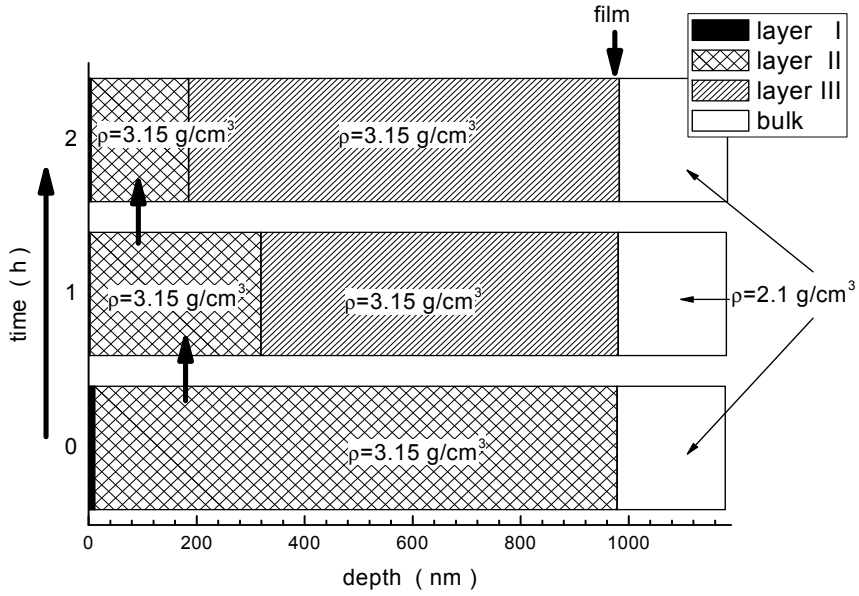

Fig. 4. Scheme of the nanostructural transformation of the GeO_2 films as a function of the depth measured from the surface of the sample and the irradiation time. As shown in this scheme, besides the silica substrate (ρ = 2.1 g/cm^3) different layers in the GeO_2 films are detected by positron spectroscopy. From the fitting of the positron data reported in Fig. 3, a density value of ρ = 3.15 g/cm^3 for the GeO_2 was obtained (see text).

#190596 - $15.00 USD Received 16 May 2013; revised 8 Jul 2013; published 30 Aug 2013

The detection by DBS of a thin superficial layer that decreases its thickness with the laser irradiation treatment, well-correlates with the results obtained by AFM. Probably, this layer is highly defected due to their S_n values by which it is characterized (higher than the S_n values found in the bulk of the films). Both the decrease in roughness and thickness of the defected superficial layer could be linked to the decrement of the attenuation coefficient. From the results reported in Table 2, it can be seen that the S_n values obtained for layer III are slightly higher than those of layer II, indicating a structural change of the GeO_2 samples. Besides, the thickness of this modified layer is larger in the sample annealed for a longer irradiation time. In the case of layer II, for the laser treated films S_n values are almost equal to that not treated sample. Figure 4 shows that: a) the bulk of the film involved by the structural change increases by increasing the irradiation time from 1 to 2 h; b) the change starts from the film/substrate interface moving towards the surface of the films. Raman spectroscopy reveals the presence of different GeO_2 phases. The rutile GeO_2 phase present after 1 h of irradiation exhibits a higher refractive index than that of the trigonal phase observed after 2 h of irradiation [40, 41]. However, DBS results would allow inferring that the lack of substantial changes in the macroscopic refractive index measured after 1 and 2 h of irradiation, respectively, could be attributed to a balance between the contributions of the different phases to the modified matrixes. The behavior described in point b) could be assigned to the heating of the substrate by the CO_2 laser inducing a progressive modification of the film from the substrate to the surface. The SiO_2 matrix, in fact, due to the lattice vibration in the region of 940 cm^{-1}, presents a higher absorbance in the region of the CO_2 laser line with respect to that of the GeO_2 system [42–44]. For that reason the CO_2 radiation is mainly absorbed by the SiO_2 substrate that induces the change in the GeO_2 film.

4. Conclusions

In the present work, a protocol to fabricate GeO_2 transparent glass ceramic planar waveguides by a Radio Frequency Sputtering technique and subsequent CO_2 laser annealing is presented. The GeO_2 planar waveguide after 2h of CO_2 laser irradiation exhibits an increase of 0.04 in the refractive index, measured at 1542 nm. Moreover, the technique of laser annealing is demonstrated to significantly reduce propagation loss in GeO_2 planar waveguides. Attenuation coefficients of 0.7 and 0.5 dB/cm at 1319 and 1542 nm, respectively, were measured after irradiation. Raman results have shown that after laser treatment for 1 h and 2 h GeO_2 nanocrystals are present with rutile and trigonal crystal phase. From AFM measurements it was found that after LA the surface roughness decreases from 1.1 to 0.7 nm. Besides, structures at nanometric scale on the surface of the samples with dimension from 10 to 50 nm attributed to the presence of GeO_2 nanocrystals were evidenced. From DBS-PAS measurements could be inferred that the structural changes inside the Germania waveguide films initiate at the film-substrate interface and propagate in the direction to the surface. This behaviour was interpreted in terms of the role of the laser heat treatment of the substrate inducing a progressive modification of the films. Additionally, from positron results a value for the density of the germania films of 3.15 ± 0.02 g/cm^3 was obtained.

Acknowledgments

This work was partially supported by Agencia Nacional de Promoción Científica y Tecnologíca (Argentina) (PICT 2011-1088), Consejo Nacional de Investigaciones Científicas y Técnicas (Argentina) (PIP # 114-200801-00444) and Progetto CNR (Italia)/CONICET (Argentina) (Project 2010-2012 and Project # IT/10/06). Part of this research was performed in the framework of the India-Trento Program for Advanced Research ITPAR Phase II research Project. The authors are grateful to Nicola Bazzanella (Università di Trento, Dipartimento di Fisica, IdEA lab.) for the EDXS measurements, Stefano Varas (IFN-CNR) for his crucial contribution in managing the rf-sputtering setup, Maurizio Mazzola (IFN-CNR) for his invaluable technical skill in CO_2 laser material processing.